Journal of Stem Cell Research

Genesis-JSCR-7(2)-88
Volume 7| Issue 2
Open Access
ISSN: 2582-8797

Differential Effects of Organ-Specific Xenogeneic Progenitor/Precursor Stem Cell Secretomes with Regeneration on Human Umbilical Vein Endothelial Cell Wound Healing

Thomas Skutella[1], Mike KS Chan[2,3*] and Dmytro Klokol[4,5]
[1]Institute for Anatomy and Cell Biology, III Medical Faculty, University of Heidelberg (Germany)
[2]European Wellness Biomedical Group (Germany, Malaysia)
[3]Baden Research & Testing Laboratories (Malaysia)
[4]European Wellness Academy (Malaysia)
[5]European Wellness Mont Kiara (Malaysia)

***Corresponding author:** Prof. Mike KS Chan, European Wellness Biomedical Group (Edenkoben, Germany)

Citation: Skutella T, Chan MKS, Klokol D. Differential Effects of Organ-Specific Xenogeneic Progenitor/Precursor Stem Cell Secretomes with Regeneration on Human Umbilical Vein Endothelial Cell Wound Healing. J Stem Cell Res. 7(2):1-22.

Received: May 22, 2026 | **Published**: June 01, 2026

Abstract

The regenerative potential of stem cell–derived secretomes has attracted increasing interest as a cell-free therapeutic strategy for tissue repair and vascular regeneration. Xenogeneic progenitor stem cells secrete a complex mixture of cytokines, growth factors, extracellular vesicles, and signaling molecules capable of modulating endothelial migration and wound healing responses. This study investigates the effects of conditioned supernatants derived from tissue-specific xenogeneic progenitor stem cell cultures on endothelial wound closure kinetics using a Human Umbilical Vein Endothelial Cell (HUVEC) scratch assay model.

Conditioned supernatants obtained from Retina, Kidney, Brain, Heart, and Thymus progenitor/precursor stem cell cultures were applied to confluent HUVEC monolayers following standardized scratch induction. A negative control group receiving basal culture medium without stem cell supernatant supplementation was included for comparative analysis. Wound closure progression was monitored over defined incubation intervals using quantitative image-based analysis to assess endothelial migration and repair dynamics.

DOI: https://doi.org/10.52793/JSCR.2026.7(2)-88

The study aims to compare the regenerative activity of tissue-specific stem cell secretomes by evaluating differences in wound closure rate, migration kinetics, and percentage area reduction relative to the control condition. It is hypothesized that stem cell supernatants will significantly enhance endothelial wound healing responses, with distinct tissue-derived secretomes exhibiting variable biological potency due to differences in paracrine factor composition.

The findings include accelerated wound closure and enhanced endothelial migration in treated groups compared with the negative control, supporting the role of xenogeneic progenitor/precursor stem cell secretomes as biologically active modulators of tissue repair. The results may contribute to the development of cell-free regenerative therapeutics and provide foundational insight into the angiogenic and reparative properties of tissue-derived stem cell conditioned media.

Keywords

Progenitor stem cells; Secretive; Exosomes; Healing; Wound closure; Regenerative medicine.

Introduction

Xenogeneic progenitor/precursor stem cells (PSC) have emerged as a promising platform in regenerative medicine due to their capacity to secrete biologically active paracrine factors that modulate tissue repair, angiogenesis, inflammation, and cellular migration. Increasing evidence suggests that the therapeutic efficacy of stem-cell–based interventions is mediated not only through direct cellular engraftment but also through the release of soluble bioactive molecules, extracellular vesicles, cytokines, growth factors, and signaling proteins collectively referred to as the stem cell secretome or conditioned supernatant [1,2]. These secreted factors may provide a cell-free therapeutic strategy with improved scalability, reduced immunogenicity, and simplified regulatory handling compared with whole-cell transplantation [3,4].

Among the in vitro methods used to evaluate regenerative potential, the Human Umbilical Vein Endothelial Cell (HUVEC) scratch assay is widely employed to investigate endothelial migration and wound closure dynamics. The assay provides a reproducible and quantitative model for studying angiogenic and wound-healing responses under controlled experimental conditions. Since endothelial migration is a critical component of tissue regeneration and neovascularization, the HUVEC scratch assay represents an effective screening platform for assessing the biological activity of stem-cell–derived supernatants [5].

In this study, wound healing activity will be evaluated following treatment with conditioned supernatants derived from PSC cultures originating from Retina, Kidney, Brain, Heart, and Thymus tissues. These tissue-specific stem cell populations are hypothesized to produce distinct secretory profiles that may differentially influence endothelial repair mechanisms. Quantitative analysis of wound closure kinetics will be performed by monitoring the rate and extent of scratch closure over time and comparing treated groups against a negative control [6].

The investigation aims to establish whether tissue-specific stem cell secretomes possess measurable pro-regenerative activity in endothelial cells and to identify which supernatants demonstrate the strongest enhancement of wound closure behavior. The findings may contribute to the development of targeted regenerative biologics and provide mechanistic insight into the therapeutic potential of xenogeneic progenitor stem cell–derived factors [7,8].

DOI: https://doi.org/10.52793/JSCR.2026.7(2)-88

Objectives of the Study

Primary objective

To quantitatively evaluate wound closure kinetics in HUVEC scratch assays following exposure to conditioned supernatants derived from xenogeneic PSC of different tissue origins (Retina, Kidney, Brain, Heart, and Thymus) compared with a negative control.

Secondary objectives

1. To determine whether tissue-specific stem cell supernatants enhance endothelial cell migration and wound closure relative to untreated controls.
2. To compare the regenerative potency of supernatants derived from different progenitor stem cell sources.
3. To assess temporal differences in wound closure rates across treatment groups through image-based quantitative analysis.
4. To identify candidate stem cell secretomes with potential angiogenic or pro-healing activity for future translational studies.

Rationalization of the experiment

In our previous works we have studied the BALB/c 3T3 Cell Transformation Assay (BALB-CTA), a validated in vitro model replicating key stages of carcinogenesis, to evaluate the tumorigenic potential of various xenogeneic progenitor stem cell cultures [14]. As a continuation of our research, we decided to explore the possible regenerative pathways and mechanisms through which PSC execute their therapeutic function. The regenerative effects of stem cells are increasingly understood to arise from paracrine signaling mechanisms rather than direct cellular replacement alone. Secreted bioactive factors from progenitor stem cells can influence endothelial proliferation, migration, extracellular matrix remodeling, and angiogenesis, all of which are essential processes in tissue repair and wound healing [9,10].

Different tissue-derived progenitor stem cells may possess unique transcriptional and secretory profiles reflective of their developmental origin and physiological function. Consequently, conditioned media obtained from Retina, Kidney, Brain, Heart, and Thymus progenitor stem cell cultures may exert differential effects on endothelial wound repair. Comparative evaluation of these secretomes is therefore necessary to identify biologically active candidates with superior regenerative properties [11].

The HUVEC scratch assay provides a cost-effective and biologically relevant model for investigating endothelial migration dynamics in response to extracellular stimuli. By introducing a standardized “wound” into a confluent endothelial monolayer and monitoring closure over time, the assay enables quantitative assessment of cellular responses to conditioned supernatants. Measuring wound closure kinetics offers a direct functional readout of the regenerative capacity of the tested secretomes [6-8,12].

Furthermore, the use of stem cell supernatants instead of live-cell therapies may reduce risks associated with cellular transplantation, including immune incompatibility, tumorigenicity, and poor engraftment efficiency. A successful demonstration of enhanced wound healing activity would support the feasibility of developing cell-free regenerative therapeutics derived from xenogeneic progenitor stem cells [13].

Expected outcomes

1. Conditioned supernatants derived from xenogeneic progenitor stem cells are expected to

DOI: https://doi.org/10.52793/JSCR.2026.7(2)-88

enhance HUVEC migration and accelerate wound closure compared with the negative control.

2. Distinct tissue-derived supernatants are anticipated to exhibit variable biological activity, reflecting differences in their secreted growth factor and cytokine composition.
3. Supernatants from highly vascularized or metabolically active tissues, such as Heart or Kidney progenitor stem cells, may demonstrate stronger pro-angiogenic and wound-healing effects.
4. Quantitative image analysis is expected to reveal statistically significant differences in:
    - Percentage wound closure
    - Migration rate
    - Time-to-closure kinetics
    - Area reduction over defined incubation periods
5. The study may identify specific progenitor stem cell secretomes suitable for further investigation as candidate regenerative biologics or angiogenic therapeutic agents.
6. The findings are expected to provide foundational data supporting the broader application of xenogeneic stem cell–derived secretomes in regenerative medicine and tissue repair research.

Materials and Methods

Experiment design

The study was designed to quantitatively evaluate endothelial wound healing responses following exposure to conditioned supernatants derived from xenogeneic progenitor stem cell cultures. Six experimental conditions were analyzed, consisting of five tissue-specific stem cell supernatants (Retina, Kidney, Brain, Heart, and Thymus) and one negative control condition. Wound healing progression was assessed using a Human Umbilical Vein Endothelial Cell (HUVEC) scratch assay with image-based computational analysis of wound closure kinetics over time [12].

HUVEC scratch assay imaging

For each experimental condition, images corresponding to four sequential timepoints were analyzed:

- h0 (baseline immediately after scratch induction)
- h16
- h24
- h48

The timepoint images for all six conditions were extracted individually from the supplied PDF dataset and processed as independent grayscale image files for quantitative analysis.

Region of interest (ROI) determination

To ensure consistency in longitudinal wound measurements, a standardized region of interest (ROI) was established for each experimental condition using the corresponding h0 image [15-17].

The initial wound corridor located between the two white guide lines was automatically identified through a multi-step image-processing workflow consisting of:

1. **Brightness Thresholding:** High-intensity pixels corresponding to the guide lines were isolated using grayscale intensity thresholding.

DOI: https://doi.org/10.52793/JSCR.2026.7(2)-88

2. **Connected-Component Analysis:** Segmented high-intensity regions were grouped into connected components to identify the two principal guide-line structures.
3. **Least-Squares Line Fitting:** Linear regression using least-squares fitting was applied to determine the orientation and position of the guide lines defining the wound corridor boundaries.

The resulting wound corridor between the fitted guide lines was designated as the ROI for that experimental condition. This identical ROI was subsequently applied to all four timepoints (h0, h16, h24, and h48) within the same condition to ensure that equivalent spatial regions were compared throughout the wound healing analysis.

Image texture analysis and wound segmentation

Within each ROI, local texture analysis was performed to distinguish cell-covered regions from the cell-free scratch area. A local texture map was generated for every image by calculating the local standard deviation of grayscale intensity values using a 15 × 15 pixel moving window [18]. This approach exploits the structural differences between cellular and non-cellular regions:

- Cell-covered regions exhibit high local texture due to the presence of cell borders, intracellular structures, and heterogeneous grayscale patterns.
- Cell-free wound regions remain comparatively smooth and display low local texture values.

A segmentation threshold was calibrated using the negative-control h0 image, where the wound area was clearly distinguishable and unambiguous. Pixels with local texture values below the calibrated threshold were classified as cell-free wound regions, whereas pixels above the threshold were classified as cell-covered regions [19,20].

To improve segmentation quality and eliminate image-processing artifacts, morphological filtering was applied:

- Small isolated objects smaller than 300 pixels were removed.
- Small holes within segmented regions smaller than 300 pixels were filled.

This process generated binary wound masks suitable for quantitative area measurements [21].

Quantitative wound area measurement

For each timepoint, the total area of cell-free pixels within the ROI was measured computationally. The measured wound area represented the remaining unhealed scratch region at each observation interval.

Wound healing progression was quantified using percentage wound closure relative to the baseline h0 condition according to the following equation:

$$\text{Closure}(t) = 100 \times \frac{\text{Free}(h0) - \text{Free}(t)}{\text{Free}(h0)}$$

Where:

- Free(h0) represents the initial cell-free wound area at baseline,

DOI: https://doi.org/10.52793/JSCR.2026.7(2)-88

- Free(t) represents the remaining cell-free wound area at timepoint t,
- Closure(t) represents the percentage of wound closure at the corresponding timepoint.

A higher percentage closure value indicates increased endothelial migration and enhanced wound healing activity.

Comparative analysis of stem cell supernatants

Quantitative wound closure kinetics were compared among all treatment groups to evaluate the regenerative potential of the tissue-specific xenogeneic progenitor stem cell supernatants. Differences in closure rates across Retina, Kidney, Brain, Heart, and Thymus conditions were analyzed relative to the negative control to determine the relative capacity of each stem cell secretome to promote endothelial repair and migration.

Results

Quantitative analysis of wound closure kinetics

The regenerative effects of xenogeneic progenitor stem cell–derived supernatants were evaluated using a quantitative Human Umbilical Vein Endothelial Cell (HUVEC) scratch assay. Wound healing progression was assessed by measuring the remaining cell-free area within the standardized region of interest (ROI) at four sequential timepoints (h0, h16, h24, and h48). Percentage wound closure was calculated relative to the initial wound area at baseline (h0), and the difference in wound closure relative to the negative control (Δ vs. negative control) was determined for each experimental condition.

The analyzed conditions included:

- Negative control
- Retina 1/4
- Kidney 2/4
- Brain 4/4
- Heart 2
- Thymus 6

Overall, all PSC supernatants demonstrated enhanced endothelial migration and accelerated wound closure compared with the negative control, particularly during later stages of the assay. The strongest regenerative responses were observed in the Brain 4/4 and Heart 2 treatment groups, both of which achieved near-complete wound closure by h48.

Table 1 summarizes the quantitative measurements of remaining cell-free area, percentage wound closure, and the difference in wound closure relative to the negative control.

Condition	Timepoint	Cell-free area (% of ROI)	Wound closure (%)	Δ vs. neg. (pp)
Negative control	h0	55.3	+0.0	**+0.0**
	h16	16.5	+70.2	**+0.0**
	h24	6.1	+89.0	**+0.0**
	h48	17.9	+67.7	**+0.0**

DOI: https://doi.org/10.52793/JSCR.2026.7(2)-88

Condition	Timepoint	Cell-free area (% of ROI)	Wound closure (%)	Δ vs. neg. (pp)
Retina 1/4	h0	68.9	+0.0	+0.0
	h16	18.1	+73.7	+3.5
	h24	9.1	+86.8	-2.1
	h48	1.1	+98.4	+30.7
Kidney 2/4	h0	69.8	+0.0	+0.0
	h16	6.0	+91.3	+21.1
	h24	4.0	+94.2	+5.2
	h48	1.3	+98.2	+30.5
Brain 4/4	h0	63.0	+0.0	+0.0
	h16	16.3	+74.1	+3.9
	h24	3.4	+94.7	+5.7
	h48	0.6	+99.0	+31.3
Heart 2	h0	67.5	+0.0	+0.0
	h16	8.1	+87.9	+17.8
	h24	1.1	+98.3	+9.4
	h48	0.5	+99.2	+31.5
Thymus 6	h0	61.3	+0.0	+0.0
	h16	16.7	+72.8	+2.6
	h24	4.9	+92.0	+3.0
	h48	6.5	+89.4	+21.7

Table 1: Remaining cell-free area and percentage wound closure per condition and timepoint. Δ denotes the difference in wound closure relative to the negative control at the same timepoint (Δ = 0.0 by definition for the negative control itself; positive values = stronger migration than control, negative values = weaker).

Comparative analysis of wound closure dynamics

Distinct differences in wound closure kinetics were observed among the tested supernatants. The negative control demonstrated progressive endothelial migration during the first 24 h, reaching 89.0% wound closure at h24; however, closure efficiency decreased by h48, where wound closure declined to 67.7%, indicating partial reopening or instability of the regenerated monolayer.

In contrast, all xenogeneic PSC supernatants maintained sustained wound closure through h48. Retina 1/4 treatment produced moderate early enhancement of migration, with wound closure reaching 73.7% at h16 and 98.4% by h48. Kidney 2/4 induced one of the most rapid early responses, achieving 91.3% closure already at h16 and 98.2% closure at h48.

DOI: https://doi.org/10.52793/JSCR.2026.7(2)-88

Brain 4/4 treatment demonstrated consistently strong regenerative activity throughout the assay. Wound closure increased from 74.1% at h16 to 94.7% at h24 and reached 99.0% by h48, corresponding to a +31.3percentage point improvement relative to the negative control.

Heart 2 produced the most pronounced overall regenerative response. This condition achieved 87.9% closure at h16, 98.3% closure at h24, and 99.2% closure at h48, representing the highest final wound closure value among all tested groups and a +31.5percentage point improvement relative to the negative control.

Thymus 6 demonstrated moderate but sustained activity, reaching 72.8% closure at h16 and 92.0% at h24. Although wound closure remained elevated at h48 (89.4%), the response was lower than that observed for Brain 4/4 and Heart 2.

Temporal migration kinetics

Analysis of temporal migration kinetics revealed that treatment-dependent differences emerged as early as h16. Kidney 2/4 and Heart 2 displayed the fastest early endothelial migration, exceeding the negative control by +21.1 and +17.8 percentage points, respectively. Brain 4/4 and Retina 1/4 produced smaller but measurable increases during the same period.

By h24, all treatment groups except Retina 1/4 exceeded the wound closure observed in the negative control. Heart 2 exhibited the largest enhancement at this timepoint (+9.4 percentage points), followed by Brain 4/4 (+5.7 percentage points) and Kidney 2/4 (+5.2 percentage points).

At h48, the divergence between treated and untreated groups became most apparent. While the negative control exhibited reduced wound closure, all treatment groups maintained high levels of closure exceeding 89%. Brain 4/4 and Heart 2 produced the strongest sustained responses, both approaching complete wound closure and exceeding the negative control by more than 31 percentage points.

Morphological and functional interpretation

The sustained reduction in cell-free area observed in treated groups suggests enhanced endothelial migration and improved stabilization of the regenerating monolayer. In contrast, the increased cell-free area observed in the negative control at h48 may indicate incomplete junctional stabilization, reduced proliferative support, or partial disruption of the newly formed endothelial layer.

The near-complete closure observed in Brain 4/4 and Heart 2 suggests that these supernatants may contain elevated concentrations of pro-regenerative signaling molecules capable of promoting endothelial motility, proliferation, and wound stabilization. Kidney 2/4 demonstrated particularly strong early migratory stimulation, whereas Retina 1/4 showed slower initial kinetics but substantial late-stage recovery.

DOI: https://doi.org/10.52793/JSCR.2026.7(2)-88

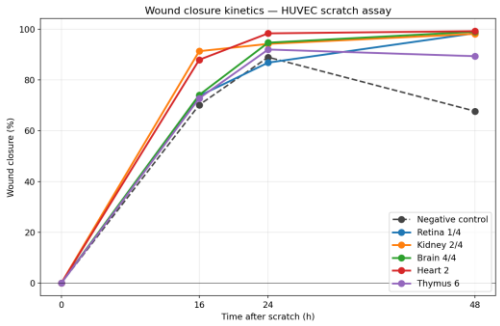

Figure 1: Wound closure (%) over time. The negative control (dashed) peaks at h24 (~89%) and drops again at h48 — likely due to partial detachment / re-opening in the absence of pro-migratory stimuli. All five supernatants drive near-complete closure at h48 (≥ 89%), with Brain 4/4 and Heart 2 reaching ≥ 99%.

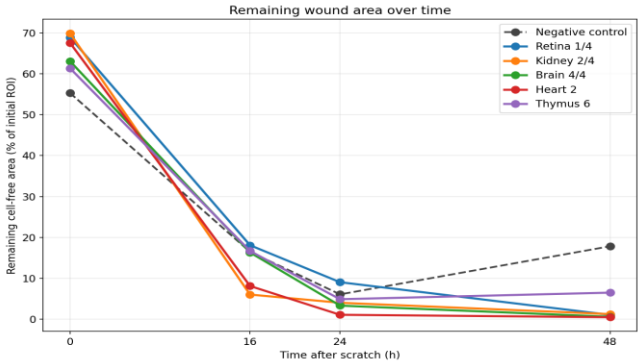

Figure 2: Remaining cell-free area (% of initial ROI). Lower values = more closed wound. Kidney 2/4 shows the fastest early closure at h16 (only ~6% residual area); Heart 2 reaches near-complete coverage by h24.

Ranking of regenerative potency

Based on final wound closure values at h48 and sustained enhancement relative to the negative control, the regenerative potency of the tested supernatants can be ranked as follows:

1. Heart 2
2. Brain 4/4
3. Retina 1/4 ≈ Kidney 2/4
4. Thymus 6
5. Negative control

When considering early migratory activity at h16, Kidney 2/4 demonstrated the most rapid initial response, followed by Heart 2.

Collectively, these results demonstrate that xenogeneic progenitor stem cell–derived supernatants significantly enhance endothelial wound healing in vitro. All tested supernatants improved wound closure kinetics relative to the negative control, with Brain 4/4 and Heart 2 producing the most robust and sustained regenerative responses. These findings support the hypothesis that tissue-specific progenitor stem cell secretomes contain bioactive factors capable of promoting endothelial regeneration and wound repair.

DOI: https://doi.org/10.52793/JSCR.2026.7(2)-88

Comparison of conditions

To evaluate the regenerative potential of the tested supernatants, wound closure was compared across all experimental conditions and benchmarked against the negative control at each observation timepoint. The analysis focused on both the absolute extent of wound closure and the relative improvement achieved by each condition over baseline untreated cells.

Absolute wound closure across conditions

Figure 3 presents the absolute wound closure percentages measured for each condition at the designated timepoints. Across the study period, all supernatant-treated groups demonstrated enhanced wound closure compared with the negative control, indicating a consistent stimulatory effect on cellular migration and repair processes.

Early-stage responses at h16 revealed notable differences in the kinetics of wound healing between conditions. Among all tested samples, Kidney 2/4 exhibited the most rapid initiation of wound closure, achieving an improvement of approximately 21 percentage points relative to the negative control. This suggests that factors present in the Kidney 2/4 supernatant may strongly promote early migratory activity or accelerate the initial phases of tissue repair. Heart 2 also demonstrated a pronounced early response, with an increase of approximately 18 percentage points above the control condition, positioning it as the second strongest performer during the early healing phase.

By h48, the differences between treated groups and the negative control became even more pronounced. All supernatants produced substantial increases in wound closure, confirming that the beneficial effects observed at h16 were sustained and amplified over time. The overall pattern indicates that while some conditions initiate repair more rapidly, all tested supernatants ultimately contribute to significantly improved wound recovery compared with untreated controls.

Relative improvement compared with the negative control

Figure 4 illustrates the difference in wound closure between each treatment condition and the negative control, expressed in percentage points. This comparative representation highlights the magnitude of the treatment effect independent of baseline closure rates.

At h48, every supernatant condition showed a clear and biologically meaningful enhancement in wound closure, with improvements ranging from +21 to +32 percentage points over the negative control. These findings indicate a robust pro-regenerative effect across all tested supernatants at later stages of healing. The relatively narrow range of improvement further suggests that the regenerative activity is consistently reproducible across multiple supernatant sources.

The early h16 timepoint revealed greater variability between conditions, allowing differentiation of the fastest-acting treatments. Kidney 2/4 emerged as the strongest early responder with a +21 percentage point advantage over the control, demonstrating rapid induction of wound repair mechanisms. Heart 2 followed closely with an increase of +18 percentage points, indicating similarly strong early regenerative activity.

These observations suggest that certain supernatants may exert distinct temporal effects on wound healing dynamics. Specifically, Kidney 2/4 appears particularly effective during the early migratory phase,

whereas other conditions may contribute more gradually but still achieve substantial closure by h48. Such temporal distinctions could reflect differences in the composition of secreted growth factors, cytokines, extracellular vesicles, or other bioactive molecules present in the supernatants.

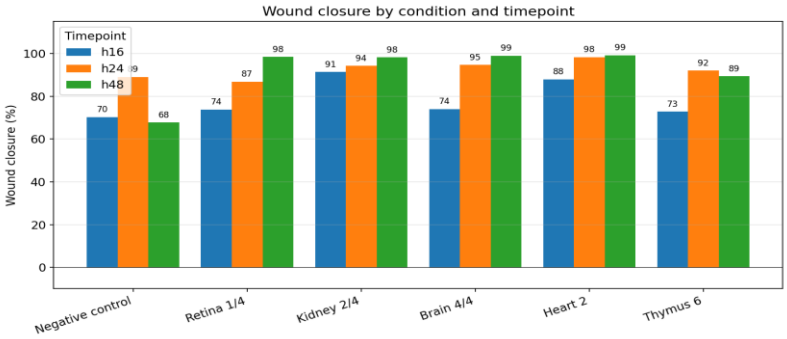

Figure 3: Absolute wound closure by condition and timepoint.

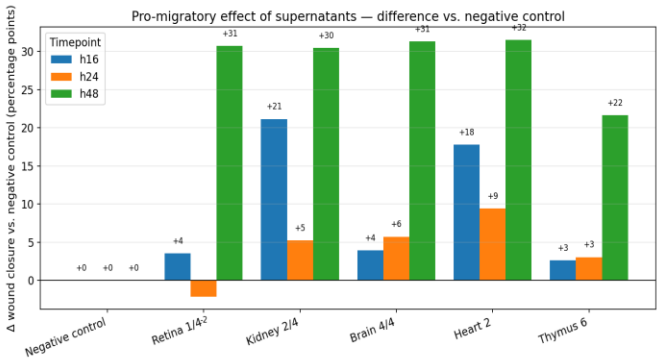

Figure 4: Difference in wound closure relative to the negative control, in percentage points. At h48 all supernatants show a clear benefit (+21 to +32 percentage points). At h16, Kidney 2/4 is the fastest early starter at +21 percentage points, followed by Heart 2 (+18).

Interpretation of healing dynamics

The comparative analysis demonstrates two important trends. First, all supernatants tested significantly enhanced wound closure relative to untreated controls, supporting the hypothesis that secreted factors derived from these tissues possess regenerative activity. Second, the rate at which this benefit emerged varied between conditions, indicating potential differences in biological potency or mechanism of action.

The strong early response observed with Kidney 2/4 may indicate the presence of signaling molecules that rapidly activate cell migration pathways, cytoskeletal remodeling, or proliferative responses. In contrast, conditions showing more moderate early activity but strong h48 performance may rely on cumulative or delayed effects associated with sustained paracrine signaling.

Overall, the data support the conclusion that tissue-derived supernatants significantly improve wound closure efficiency, with Kidney 2/4 and Heart 2 demonstrating particularly strong early-stage activity. The sustained enhancement observed at h48 across all conditions further emphasizes the therapeutic potential of these secreted biological factors in regenerative and wound-healing applications.

DOI: https://doi.org/10.52793/JSCR.2026.7(2)-88

Per-timepoint comparison vs. control

To better characterize the temporal dynamics of wound healing, each conditioned-medium sample was compared directly against the negative control at every observation timepoint (h16, h24, and h48). In the graphical representation, the dashed reference line indicates the closure achieved by the negative control, allowing rapid visual assessment of treatment-associated enhancement or decline. Teal bars represent conditions exceeding the control, whereas magenta bars indicate values below the control threshold, if present. The accompanying quantitative table summarizes the absolute wound closure percentage, the difference relative to the control in percentage points, and the fold-change compared with untreated HUVEC cultures.

Baseline behavior of the negative control

The negative control provides an important reference for intrinsic migratory behavior in the absence of exogenous growth-promoting factors. Untreated HUVECs were capable of partial wound closure through spontaneous migration alone, reaching approximately 70% closure at h16 and increasing further to approximately 89% at h24. This indicates that endothelial cells retain a substantial endogenous capacity for gap closure under standard culture conditions.

However, by h48 the closure rate declined again to approximately 68%, indicating that the initially formed monolayer was not stably maintained over time. Microscopic evaluation of the h48 control image visually confirmed partial disruption of the cellular monolayer, including detachment of individual cells and reappearance of open wound regions. These observations suggest that, in the absence of supportive trophic factors, intrinsic migration alone is insufficient to sustain long-term wound stability and cohesive monolayer integrity.

Overall effect of conditioned supernatants

In contrast to the negative control, all five conditioned-medium supernatants markedly enhanced wound closure and promoted more stable repair behavior. At the h48 endpoint, every supernatant-treated condition achieved at least 89% closure, whereas the untreated control remained at only approximately 68%. This corresponds to measurable advantages ranging from +22 to +32 percentage points, demonstrating a robust stimulatory effect on endothelial regeneration.

The data indicate that conditioned media not only accelerate migration but also appear to stabilize the repaired monolayer over prolonged incubation periods. Compared with the instability observed in untreated cells, supernatant-treated cultures maintained near-complete closure and preserved structural continuity at later stages of healing.

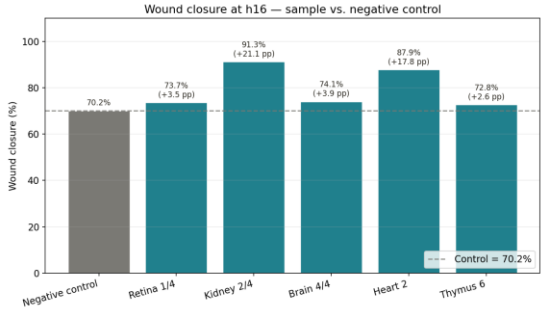

DOI: https://doi.org/10.52793/JSCR.2026.7(2)-88

Figure 5: Wound closure at h16. Dashed line = negative control (70.2%). Teal bars = sample exceeds control; magenta bars = sample below control. Values above each bar give the absolute closure and the difference vs. control in percentage points.

Condition	Wound closure (%)	Δ vs. control (pp)	Fold vs. control
Negative control (reference)	**70.2**	+0.0	**1.00 ×**
Retina 1/4	73.7	**+3.5**	1.05 ×
Kidney 2/4	91.3	**+21.1**	1.30 ×
Brain 4/4	74.1	**+3.9**	1.06 ×
Heart 2	87.9	**+17.8**	1.25 ×
Thymus 6	72.8	**+2.6**	1.04 ×

Table 2: h16: sample vs. negative control. Δ = sample − control (percentage points); fold = sample / control.

Early phase response (h16): fastest initiators of migration

The h16 timepoint revealed substantial differences in the speed of initial wound response between supernatants. Among all tested conditions, Kidney 2/4 displayed the most pronounced early activity, exceeding the negative control by approximately +21 percentage points. This strong early advantage identifies Kidney 2/4 as the fastest initiator of endothelial migration and suggests the presence of highly potent pro-migratory signaling factors.

Heart 2 also demonstrated a clearly accelerated response, reaching approximately +18 percentage points above the control condition at h16. Although slightly less pronounced than Kidney 2/4, the Heart 2 supernatant similarly promoted rapid activation of wound closure pathways during the earliest phase of repair.

By comparison, Brain 4/4, Retina 1/4, and Thymus 6 showed only modest early improvements over baseline, each exceeding the control by approximately +3 to +4 percentage points. These results suggest that their biological effects emerge more gradually, potentially relying on sustained signaling mechanisms rather than immediate migratory activation.

The distinction between rapid and delayed responders highlights important temporal differences in regenerative behavior and may reflect variation in the molecular composition of the individual supernatants.

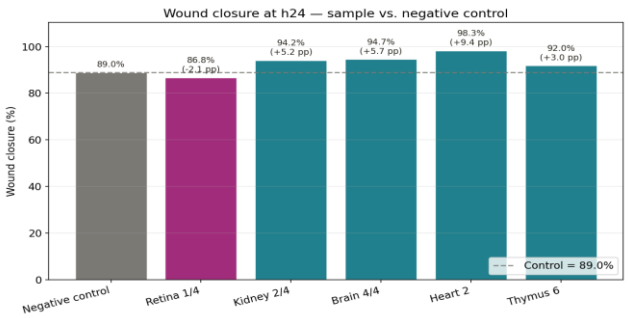

DOI: https://doi.org/10.52793/JSCR.2026.7(2)-88

Figure 6: Wound closure at h24. Dashed line = negative control (89.0%). Teal bars = sample exceeds control; magenta bars = sample below control. Values above each bar give the absolute closure and the difference vs. control in percentage points.

Condition	Wound closure (%)	Δ vs. control (pp)	Fold vs. control
Negative control (reference)	**89.0**	+0.0	**1.00 ×**
Retina 1/4	86.8	**-2.1**	0.98 ×
Kidney 2/4	94.2	**+5.2**	1.06 ×
Brain 4/4	94.7	**+5.7**	1.06 ×
Heart 2	98.3	**+9.4**	1.11 ×
Thymus 6	92.0	**+3.0**	1.03 ×

Table 3: h24: sample vs. negative control. Δ = sample − control (percentage points); fold = sample / control.

Late phase response (h48): near-complete wound closure

At the final h48 timepoint, the regenerative potential of all supernatants became fully apparent. Brain 4/4 and Heart 2 achieved nearly complete closure, reaching 99.0% and 99.2%, respectively. These values indicate essentially total restoration of the endothelial monolayer and represent the strongest overall endpoint performance among all tested conditions.

Retina 1/4 and Kidney 2/4 followed closely behind, reaching 98.4% and 98.2% closure, respectively. Although marginally lower than Brain 4/4 and Heart 2, these values still indicate exceptionally efficient wound repair and sustained monolayer stability.

Thymus 6 achieved a comparatively lower endpoint value of 89.4%. While this still substantially exceeded the negative control, the condition exhibited evidence of slight wound re-opening between h24 (92%) and h48. This decline may indicate reduced stability of cell adhesion, weaker proliferative support, or less durable maintenance of the repaired monolayer. The partial regression contrasts with the stable or continuously improving closure observed in the other supernatant-treated groups.

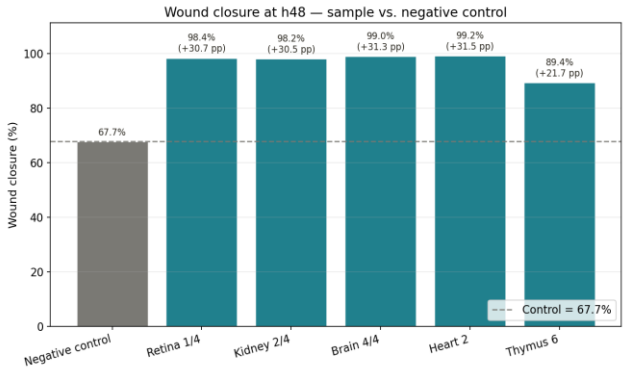

Figure 7: Wound closure at h48. Dashed line = negative control (67.7%). Teal bars = sample exceeds control;

DOI: https://doi.org/10.52793/JSCR.2026.7(2)-88

magenta bars = sample below control. Values above each bar give the absolute closure and the difference vs. control in percentage points.

Condition	Wound closure (%)	Δ vs. control (pp)	Fold vs. control
Negative control (reference)	**67.7**	+0.0	**1.00 ×**
Retina 1/4	98.4	**+30.7**	1.45 ×
Kidney 2/4	98.2	**+30.5**	1.45 ×
Brain 4/4	99.0	**+31.3**	1.46 ×
Heart 2	99.2	**+31.5**	1.47 ×
Thymus 6	89.4	**+21.7**	1.32 ×

Table 4: h48: sample vs. negative control. Δ = sample − control (percentage points); fold = sample / control.

Endpoint ranking of regenerative performance

Based on wound closure efficiency at h48, the overall ranking of regenerative activity can be summarized as follows:

Heart 2 ≈ Brain 4/4 > Retina 1/4 ≈ Kidney 2/4 >> Thymus 6 > Negative Control

Heart 2 and Brain 4/4 emerged as the highest-performing conditions, achieving essentially complete wound closure with excellent late-stage stability. Retina 1/4 and Kidney 2/4 demonstrated nearly equivalent endpoint performance, although Kidney 2/4 distinguished itself through exceptionally rapid early migration. Thymus 6, while still beneficial compared with the untreated control, displayed comparatively weaker long-term stability.

Taken together, these findings demonstrate that all conditioned supernatants significantly improve endothelial wound healing compared with intrinsic migration alone. The data further suggest that distinct supernatants may preferentially influence different phases of the regenerative process, with some acting as rapid initiators of migration and others supporting sustained closure and long-term monolayer integrity.

Discussion

The present study demonstrates that conditioned supernatants derived from progenitor stem cell cultures significantly enhance endothelial wound closure compared with untreated controls, supporting the concept that stem cell–associated secretomes possess potent regenerative activity. Across all evaluated conditions, treated HUVEC monolayers exhibited accelerated migration, improved wound coverage, and superior long-term stability relative to cells maintained without growth-promoting factors. Importantly, the observed regenerative effects were not limited to a single tissue source, suggesting that multiple progenitor-derived secretomes contain biologically active factors capable of stimulating endothelial repair processes.

DOI: https://doi.org/10.52793/JSCR.2026.7(2)-88

The comparative analysis further revealed distinct temporal healing patterns among the tested supernatants, indicating that different progenitor cell populations may secrete unique combinations of trophic molecules that influence specific phases of tissue regeneration. Some supernatants preferentially enhanced early migration kinetics, whereas others promoted sustained closure and long-term monolayer stability. These findings are highly relevant for regenerative medicine because effective tissue repair requires coordinated activation of multiple biological pathways, including cell migration, proliferation, extracellular matrix remodeling, angiogenesis, and survival signaling.

The negative control condition established the intrinsic migratory behavior of endothelial cells in the absence of exogenous regenerative stimuli. HUVEC monolayers were capable of partial spontaneous wound closure, reaching approximately 70% closure at h16 and increasing further to approximately 89% at h24. This confirms that endothelial cells possess an inherent capacity for migration and partial self-repair under standard culture conditions.

However, the untreated monolayer failed to maintain stable closure over prolonged incubation. By h48, wound closure declined to approximately 68%, accompanied by visible monolayer disruption and detachment of individual cells. This regression strongly suggests that intrinsic migration alone is insufficient to sustain long-term endothelial integrity. Without trophic support, cells may undergo stress-related detachment, reduced adhesion, cytoskeletal destabilization, or apoptosis, ultimately compromising monolayer continuity.

The instability observed in untreated cultures highlights the importance of extracellular signaling molecules in vascular repair. In vivo, endothelial healing is tightly regulated by paracrine factors released from surrounding stromal cells, immune cells, and progenitor populations. The absence of such signaling in the negative control likely contributed to impaired long-term maintenance of the repaired area.

In contrast to the untreated control, all conditioned supernatants markedly enhanced wound closure and preserved monolayer integrity throughout the experimental period. By h48, every supernatant-treated condition achieved at least 89% closure, corresponding to improvements of approximately +22 to +32 percentage points relative to control cultures.

These findings strongly support the hypothesis that PSC exert regenerative effects primarily through paracrine signaling mechanisms mediated by their secretome. Increasing evidence in regenerative biology indicates that many therapeutic benefits traditionally attributed to stem cell engraftment are in fact mediated by bioactive molecules secreted into the extracellular environment. These include growth factors, cytokines, chemokines, extracellular vesicles, exosomes, microRNAs, lipid mediators, and matrix-remodeling enzymes.

The observed enhancement of endothelial migration likely reflects coordinated activation of multiple signaling pathways involved in tissue repair. Candidate mediators may include vascular endothelial growth factor (VEGF), fibroblast growth factors (FGFs), hepatocyte growth factor (HGF), transforming growth factor-β (TGF-β), platelet-derived growth factor (PDGF), stromal-derived factor-1 (SDF-1), and insulin-like growth factor (IGF). These molecules are known to stimulate endothelial motility, proliferation, cytoskeletal remodeling, and angiogenic activity.

In addition to soluble growth factors, extracellular vesicles and exosomes released by PSC may contribute

substantially to the regenerative response. Exosomes can transfer proteins, messenger RNAs, microRNAs, and regulatory signaling molecules directly into recipient cells, thereby modulating gene expression and cellular behavior. Such vesicle-mediated communication has emerged as a central mechanism in stem cell–driven tissue regeneration.

The temporal analysis revealed major differences in early wound-healing kinetics between supernatants. Kidney 2/4 demonstrated the strongest early response, exceeding the negative control by approximately +21 percentage points at h16. This identifies Kidney 2/4 as the most potent early initiator of endothelial migration among the tested conditions.

Heart 2 also induced pronounced early acceleration, improving closure by approximately +18 percentage points relative to control. These observations suggest that both Kidney 2/4 and Heart 2 secretomes contain particularly high concentrations of rapid-response pro-migratory factors.

One possible explanation is enhanced activation of pathways regulating cytoskeletal dynamics and focal adhesion turnover. Endothelial migration requires coordinated remodeling of actin filaments, lamellipodia formation, and integrin-mediated adhesion. Secreted molecules such as VEGF and HGF can rapidly activate intracellular signaling cascades including PI3K/Akt, MAPK/ERK, and focal adhesion kinase (FAK), thereby accelerating directed migration toward the wound area.

Another potential contributor may be the presence of extracellular vesicles enriched in migration-associated microRNAs. Specific microRNAs transported through exosomes have been shown to promote endothelial motility, suppress apoptosis, and enhance angiogenesis. The particularly strong early effect observed with Kidney 2/4 may therefore reflect an especially potent exosomal signaling profile.

By contrast, Brain 4/4, Retina 1/4, and Thymus 6 produced only modest improvements during the early phase, exceeding control levels by approximately +3 to +4 percentage points at h16. While initially slower, these conditions later achieved near-complete closure, suggesting that their regenerative activity may rely more heavily on sustained proliferative or stabilizing mechanisms rather than immediate migratory activation.

At the h48 endpoint, the regenerative potential of all conditioned supernatants became fully apparent. Heart 2 and Brain 4/4 achieved nearly complete closure, reaching 99.2% and 99.0%, respectively. Retina 1/4 and Kidney 2/4 followed closely with 98.4% and 98.2% closure.

These findings indicate not only accelerated migration but also durable stabilization of the repaired endothelial layer. Stable wound closure requires maintenance of cell-cell junctions, extracellular matrix interactions, and endothelial barrier integrity. The superior performance of treated cultures therefore suggests that progenitor secretomes support long-term cellular cohesion and survival in addition to initial migration.

The particularly strong endpoint performance of Brain 4/4 may reflect the presence of neurotrophic or anti-inflammatory factors that improve long-term cell viability and reduce stress-induced detachment. Neural-derived progenitor cells are known to secrete molecules capable of enhancing tissue protection, reducing oxidative stress, and modulating inflammatory signaling, all of which may contribute to sustained monolayer integrity.

DOI: https://doi.org/10.52793/JSCR.2026.7(2)-88

Thymus 6 displayed comparatively weaker long-term stability, with closure decreasing slightly from approximately 92% at h24 to 89.4% at h48. Although still markedly superior to the negative control, this partial regression may indicate reduced support for proliferative maintenance or weaker stabilization of intercellular adhesion complexes. The observation underscores that regenerative efficiency depends not only on the speed of migration but also on the capacity to maintain structural integrity over time.

Implications for Regenerative Medicine

The results of this study have important implications for the development of cell-free regenerative therapies. Traditional stem cell therapies face several practical and biological challenges, including immune compatibility, limited engraftment efficiency, risk of uncontrolled differentiation, tumorigenicity, and difficulties in long-term storage and transport. Secretome-based therapies may overcome many of these limitations while preserving much of the regenerative benefit associated with stem cells.

Conditioned media and extracellular vesicle preparations derived from progenitor stem cells represent highly attractive therapeutic platforms because they can deliver complex regenerative signaling without requiring direct cell transplantation. Such approaches may offer improved safety, easier standardization, reduced immunogenicity, and greater scalability for clinical applications.

The strong enhancement of endothelial repair observed in this study is particularly relevant for vascular regeneration and ischemic tissue repair. Endothelial dysfunction contributes to impaired healing in numerous pathological conditions, including diabetic ulcers, cardiovascular disease, peripheral ischemia, chronic inflammatory disorders, and post-surgical tissue injury. Secretome-based therapies capable of restoring endothelial migration and vascular integrity could therefore provide substantial clinical benefit.

Beyond vascular repair, progenitor stem cell secretomes may have broad applications in organ and tissue regeneration. Their complex mixture of growth-promoting and immunomodulatory factors could support regeneration in cardiac tissue following myocardial infarction, neural tissue after neurodegenerative injury, renal tissue following ischemic damage, retinal degeneration, and musculoskeletal injuries. Tissue-specific progenitor secretomes may eventually be optimized to target particular regenerative pathways depending on the clinical application.

Future perspectives

The differential behavior observed between supernatants highlights the need for further molecular characterization of progenitor-derived secretomes. Proteomic, transcriptomic, and extracellular vesicle analyses could help identify the key bioactive components responsible for rapid migration, sustained proliferation, or monolayer stabilization.

Future studies should also investigate the signaling pathways activated in recipient endothelial cells following exposure to specific supernatants. Understanding the mechanistic basis of these regenerative effects may enable development of optimized secretome formulations with enhanced therapeutic potency.

Additionally, translation toward clinical application will require evaluation in more complex experimental systems, including three-dimensional tissue models and in vivo injury models. Standardization of secretome production, dosing, purification, and storage conditions will also be essential for therapeutic implementation.

DOI: https://doi.org/10.52793/JSCR.2026.7(2)-88

Conclusion

Overall, the present findings demonstrate that progenitor stem cell–derived conditioned supernatants significantly enhance endothelial wound healing compared with intrinsic migration alone. All tested supernatants promoted substantial improvements in wound closure, while Heart 2 and Brain 4/4 achieved the strongest late-stage regenerative performance and Kidney 2/4 displayed the fastest early migratory activation.

The data strongly support a paracrine mechanism of action mediated through the progenitor stem cell secretome, including growth factors, cytokines, extracellular vesicles, and regulatory signaling molecules. These secreted components appear capable of accelerating migration, stabilizing endothelial monolayers, and sustaining long-term tissue repair.

Taken together, the results highlight the considerable promise of progenitor stem cell secretomes as next-generation tools for regenerative medicine, vascular repair, and tissue engineering. Their potent biological activity, combined with the advantages of cell-free therapeutic strategies, positions secretome-based approaches as highly promising candidates for future clinical translation in organ and tissue regeneration.

Limitations of the Study

Despite the clear and consistent differences observed between conditioned supernatants and the negative control, several methodological limitations must be considered when interpreting the present results. These limitations primarily relate to the nature of the image data, the quantification approach, and the absence of biological replication at a scale sufficient for formal statistical inference.

The analysis was performed on JPEG images embedded within a PDF document. As a result, the raw dataset is inherently rasterized and compressed, which introduces potential loss of fine structural detail. Each condition and timepoint is represented by a single field of view (n = 1), limiting spatial representation of the wound area.

This sampling density is insufficient to capture intra-well heterogeneity, which is commonly observed in scratch assays due to variations in cell density, edge effects, and local microenvironmental differences. Consequently, the reported values should be interpreted as representative snapshots rather than comprehensive population-level measurements.

Due to the absence of biological and technical replicates, statistical analyses such as mean ±standard error of the mean (SEM), confidence intervals, or inferential tests (e.g., ANOVA or mixed-effects modeling) could not be performed. The dataset therefore supports only descriptive comparisons between conditions.

While the magnitude and consistency of observed effects, particularly the strong separation between treated conditions and the negative control, suggest robust biological trends, the lack of replication prevents formal quantification of variability and statistical significance. As such, conclusions are necessarily qualitative to semi-quantitative rather than inferential.

Wound closure was quantified using a texture-based segmentation approach that distinguishes cell-free regions from cell-covered areas based on local brightness variance. While this method performs well for clearly defined wound boundaries, it has inherent limitations in detecting sparsely distributed or

morphologically subtle cellular structures.

In particular, thinly spread or highly migratory individual cells at the wound edge may be underestimated or partially excluded from the segmentation mask. This could lead to a slight underestimation of true cell coverage, especially during early migration phases when cells are dispersed and not yet forming continuous monolayers.

Additionally, variations in illumination, focus, or image contrast can influence segmentation accuracy, potentially introducing small systematic biases across conditions or timepoints.

A key limitation of the present dataset is the lack of biological replication. Publication-grade wound healing assays typically require a minimum of three biological replicates, with multiple technical replicates and several fields of view per well (e.g., ≥ 3 wells and ≥ 3 fields per well). This design enables robust estimation of variability and ensures that observed effects are reproducible across independent experimental units.

Without such replication, it is not possible to assess inter-experimental variability, batch effects in supernatant preparation, or potential differences in cell seeding density and growth conditions. Consequently, the current findings should be interpreted as preliminary and hypothesis-generating rather than definitive.

Another important limitation relates to the lack of standardized imaging acquisition metadata. For optimal comparability in time-lapse wound healing studies, images should be acquired under strictly controlled and identical conditions, including consistent focus, exposure time, illumination intensity, and microscope calibration across all timepoints.

Any variation in imaging parameters may influence perceived wound area and segmentation output, particularly in brightness-based analysis workflows. While the present dataset shows clear and biologically plausible trends, minor technical variability cannot be excluded as a contributing factor to small differences between conditions.

In summary, the study provides strong descriptive evidence that progenitor stem cell–derived supernatants enhance endothelial wound closure. However, the conclusions are constrained by the use of single-field, non-replicated image data, absence of statistical testing, and potential limitations of the segmentation method and imaging consistency.

Future studies should address these limitations through inclusion of biological replicates, standardized imaging protocols, and statistically powered experimental designs. Such improvements would enable more rigorous quantification of effect sizes, variability, and mechanistic interpretation, thereby strengthening the translational relevance of the findings.

Conflicts of interest

Authors declare no conflicts of interest.

Appendix — segmentation QC

The overview below shows for every image the detected ROI (red outlines) and the area classified as cell-free (green), allowing visual confirmation that the quantification follows the biological impression.

DOI: https://doi.org/10.52793/JSCR.2026.7(2)-88

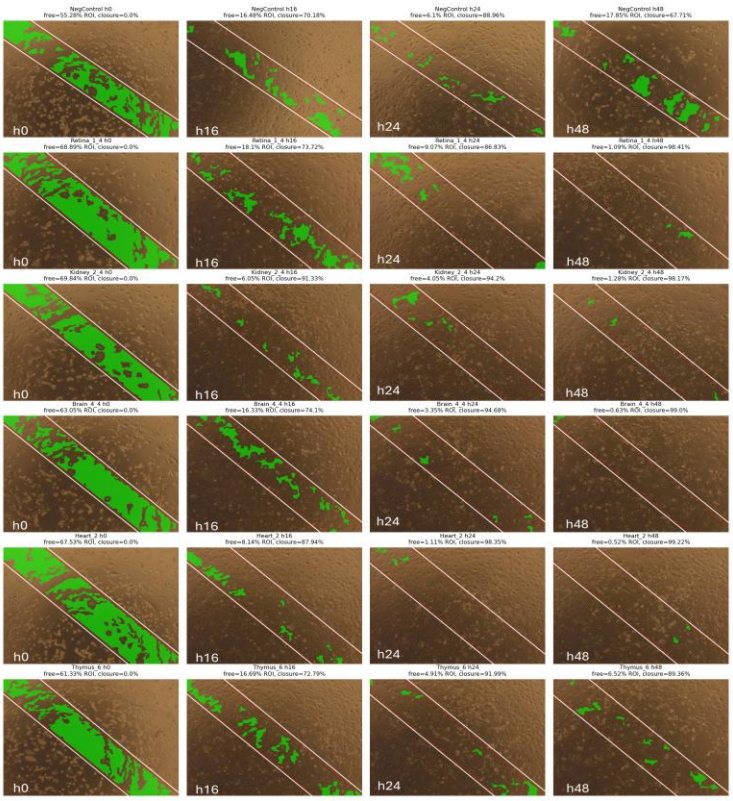

References

1. Camussi G, Deregibus MC, & Cantaluppi V. (2013) Role of stem-cell-derived microvesicles in the paracrine action of stem cells. Biochemical Society Transactions. 41(1):283-87.
2. Sun DZ, Abelson B, Babbar P, Damaser MS, et al. (2019) Harnessing the mesenchymal stem cell secretome for regenerative urology. Nature Reviews Urology. 16:363-75.
3. Yin L, Liu X, Shi Y, Ocansey DKW, Hu Y, et al. (2020) Therapeutic advances of stem cell-derived extracellular vesicles in regenerative medicine. Cells. 9(3):707.
4. Zhou C, Zhang B, Yang Y, Jiang Q, Li T, et al. (2023) Stem cell-derived exosomes: Emerging therapeutic opportunities for wound healing. Stem Cell Res Thera. 14:107.
5. Liang CC, Park AY, & Guan JL. (2007) In vitro scratch assay: A convenient and inexpensive method for analysis of cell migration in vitro. Nature Protocols. 2(2):329-33.
6. Rodriguez LG, Wu X, Guan JL. (2005) Wound-healing assay. In Methods in Mole Bio. 294:23-29.
7. Cory G. (2011) Scratch-wound assay. Methods in Mole Bio. 769:25-30.
8. Staton CA, Reed MW, Brown NJ. (2009) A critical analysis of current in vitro and in vivo angiogenesis assays. Inte J Exper Pathol. 90(3):195-21.
9. Gnecchi M, He H, Liang OD, Melo LG, Morello F, et al. (2005) Paracrine action accounts for marked protection of ischemic heart by Akt-modified mesenchymal stem cells. Nature Med. 11(4):367-68.
10. Maacha S, Sidahmed H, Jacob S, Gentilcore G, Calzone R, et al. (2020) Paracrine mechanisms of mesenchymal stromal cells in angiogenesis. Stem Cells Inte. 2020:4356359.
11. Teixeira FG, Carvalho MM, Panchalingam KM, Rodrigues AJ, Mendes-Pinheiro B, et al. (2017) Impact of the secretome of human mesenchymal stem cells on brain structure and function. Stem Cell Rep. 8(5):1280-94.
12. Liang CC, Park AY, Guan JL. (2007) In vitro scratch assay: A convenient and inexpensive method for analysis of cell migration in vitro. Nature Protocol. 2(2):329-33.

DOI: https://doi.org/10.52793/JSCR.2026.7(2)-88

13. Baraniak PR, McDevitt TC. (2010) Stem cell paracrine actions and tissue regeneration. Reg Med. 5(1):121-143.
14. Chan MK, Wong MB, Pan SY, Chernykh V, Shyshkina N, et al. (2025) Carcinogenicity and Oncogenicity of Precursor/Progenitor Stem Cells of the Xenogeneic Origin: The Balb/C-3t3 Cell Transformation Assay. SSP Modern Pharm Med. 5(3):20-37.
15. Otsu N. (1979) A threshold selection method from gray-level histograms. IEEE Transactions on Systems, Man, and Cybernetics. 9(1):62-66.
16. Szeliski R. (2022) Computer vision: Algorithms and applications (2nd ed) Springer.
17. Gonzalez RC, Woods RE. (2018) Digital image processing (4th ed).
18. Burger W, Burge MJ. (2016) Digital image processing: An algorithmic introduction using Java (2nd ed.). Springer.
19. Haralick RM, Shanmugam K, Dinstein I. (1973) Textural features for image classification. IEEE Transactions on Systems, Man, and Cybernetics. SMC-3(6):610-21.
20. Soille P. (2003) Morphological image analysis: Principles and applications (2nd ed.). Springer.
21. Burger W, Burge MJ. (2016) Digital image processing: An algorithmic introduction using Java (2nd ed.). Springer.